

X-ray diffraction studies of ordered chloride and bromide monolayers at the Au(111)-solution interface

O. M. Magnussen and B. M. Ocko

Department of Physics, Brookhaven National Laboratory, Upton, New York 11973

R. R. Adzic and J. X. Wang

Department of Applied Science, Brookhaven National Laboratory, Upton, New York 11973

(Received 11 October 1994)

We present *in situ* surface x-ray scattering observations of ordered chloride and bromide monolayers on Au(111) electrodes in aqueous solutions as an example of *in situ* x-ray diffraction from adsorbates of the lighter elements ($Z < 50$). At a critical surface density both halides form incommensurate, hexagonal-close-packed monolayers that compress uniformly with increasing potential. Our structural results provide quantitative data on the residual adsorbate charge, the two-dimensional melting, and the two-dimensional compressibilities of halide monolayers.

The adsorption of halogen gases on metal surfaces and of halide anions on metal electrodes in aqueous solutions has been extensively studied in the past. In a vacuum environment, chemisorbed halogens dissociate and form ordered monolayers.¹ These adlayers are often incommensurate (no lateral registry) with the metal substrate and change continuously with increasing halogen coverage, not unlike the two-dimensional phases of physisorbed noble gases.² However, the equilibrium properties of halide adlayers are difficult to obtain in vacuum experiments due to the strong chemical halide-metal interaction. In contrast, equilibrium is readily established at the liquid-solid interface where the chemical potential of the adsorbate can be controlled via the electrode potential. With the recent advent of modern *in situ* techniques the structure of these interfaces can now be determined. Studies by *in situ* scanning tunneling microscopy (STM) and surface x-ray scattering revealed that the strongly bound iodide ions form close-packed, ordered monolayers on gold and platinum electrodes.³⁻⁶ Much less is known about the lighter halides. Ordered bromide adlayers were found in only one preliminary STM study⁵ and ordered phases of chloride and fluoride anions at a solid-liquid interface have not been observed to our knowledge. Here we report *in situ* observations of ordered chloride and bromide monolayers on Au(111) by grazing incident angle x-ray diffraction. The evaluated equilibrium properties of halide monolayers will be compared to those of noble gas and metallic adlayers.

Grazing incident angle x-ray diffraction measurements of the interface structure of Au(111) electrodes were carried out at beamline X22B at the National Synchrotron Light Source at a wavelength $\lambda = 1.54 \text{ \AA}$. The experiments were performed on Au(111) single crystals sputtered and annealed at 1000 K in vacuum or prepared by flame annealing. The sample was then mounted in an electrochemical cell that was filled with deaerated suprapur 0.1M HClO₄ solutions containing NaCl or NaBr in the range 0.001–1M. Subsequently the cell was deflated leaving an electrolyte film of $\approx 10 \mu\text{m}$ thickness between the Au(111) surface and the 4- μm -thick prolene (Chemplex®) x-ray window. During the experiment the

cell was surrounded by a N₂ atmosphere to keep the electrolyte free of oxygen. The electrode potential was controlled versus a Ag/AgCl (3M KCl) reference electrode. For further experimental details see Refs. 6 and 7.

First we will describe the experiments in chloride solution. At 0.3 V diffraction peaks are only observed at the positions of the crystal truncation rods [open circles in Fig. 1(a)]. They are indexed by integer reflections, i.e., (1,0), (0,1), etc., in the employed hexagonal coordinate system.^{6,7} After increasing the potential to values posi-

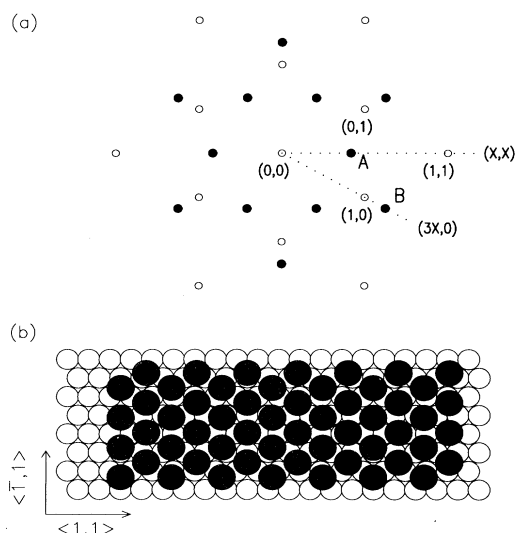


FIG. 1. (a) In-plane x-ray diffraction pattern of a Au(111) electrode in 0.1M HClO₄ + x M NaCl ($0.001 < x < 1$). Diffraction peaks at the positions of the crystal truncation rods (open circles) result from the hexagonal Au(111) substrate and are observed at all electrode potentials. At potentials above 0.68 V superstructure peaks (filled circles) appear at the (X,X) positions (A) and the $(3X,0)$ positions (B) with $0.405 \leq X \leq 0.422$. (b) Real-space model of the corresponding incommensurate adlayer structure; Au surface atoms and adsorbed chloride ions are indicated by open and filled circles, respectively.

tive of 0.68 V (for 0.1M NaCl) we observe distinct changes in the diffracted x-ray intensities. The diffraction pattern in this potential regime, shown in Fig. 1(a), exhibits additional peaks at the $\{X,X\}$ positions, where X is dependent on potential and NaCl concentration and ranges between 0.405 and 0.422. Beside these strong first-order reflections, weaker second-order reflections were observed at the $\{3X,0\}$ positions. These diffraction peaks indicate the formation of an ordered monolayer of adsorbed chloride on the gold substrate. Both the chloride (filled circles) and the underlying gold (open circles) diffraction pattern are hexagonal and rotated with respect to each other by 30° . The corresponding chloride adlayer forms an aligned, hexagonal close-packed structure, as displayed in Fig. 1(b), which is incommensurate with the gold lattice.

Figure 2 shows typical x-ray scattering intensity profiles at the position of the chloride-adlayer peaks. At an electrode potential of 0.72 V pronounced peaks in the scattered intensity are observed. In contrast, only a uniform background is measured in profiles obtained at 0.3 V, where the surface concentration of adsorbed chloride is lower and the adlayer apparently is disordered. The radial half width at half maximum (HWHM) of the superstructure peaks is 0.003 \AA^{-1} , the angular HWHM in the corresponding φ -angle scans (i.e., perpendicular to the radial direction) is 0.1° . By neglecting the limited resolution and assuming a perfect sample mosaic a lower bound on the coherence length of 500 \AA is obtained from the latter peak width. This indicates a well-ordered chloride adlayer with domains of similar size as the atomically flat

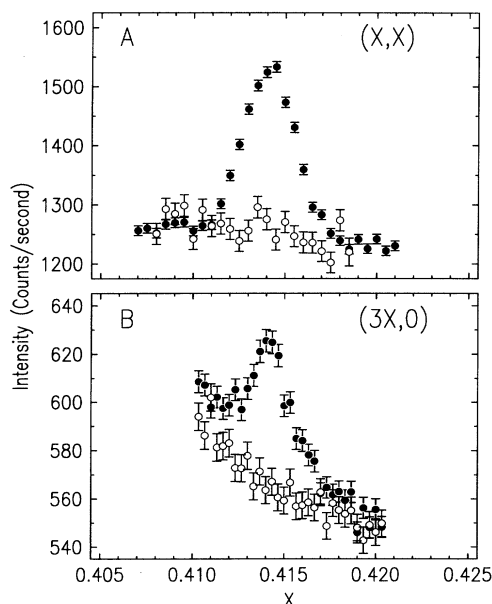


FIG. 2. X-ray scattering profiles along (X,X) and $(3X,0)$ in the range $0.410 < X < 0.425$ [directions indicated by dotted lines in Fig. 1(a)] of Au(111) in 0.1M HClO₄+0.1M NaCl at 0.3 V (open circles) and 0.72 V (filled circles). The peaks at 0.72 V correspond to the first- and second-order reflections of the adlayer structure, depicted in Fig. 1(a) by A and B, respectively (measured at a grazing incident angle of 1.25°).

terraces of the underlying Au(111) surface.⁷

The observation of diffraction peaks resulting from an ordered chloride adlayer demonstrates the ability of *in situ* x-ray techniques to obtain information on low- Z adsorbates. In comparison to vacuum measurements, the background intensity in studies at solid-liquid interfaces is enhanced due to diffuse scattering from the bulk electrolyte and the window material, which is an inherent limitation. To date, in-plane diffraction peaks have been reported only for ordered adlayers of high- Z atoms (atomic number $Z > 50$) such as lead,⁸ thallium,⁹ gold,⁷ or iodide,⁶ where the peak intensity is two to ten times higher than the background. Since the scattered intensity is proportional to the square of the number of electrons, scattering from a chloride adlayer (with $Z_{\text{Cl}}=17$) is about an order of magnitude weaker. As a result the signal-to-background ratio is lower than 1:4. Our observation increases the prospects for surface x-ray scattering as a tool for future *in situ* studies of ionic and organic adlayers.

The chloride surface density Γ and the chloride coverage θ relative to the Au substrate, respectively, can be directly computed from the position of the lowest-order diffraction peak. The chloride adlayer and the Au substrate lattice are characterized by the length of nearest-neighbor distances (a_{Cl} and $a_{\text{Au}}=2.885 \text{ \AA}$) or the corresponding values in reciprocal space (a_{Cl}^* and a_{Au}^*). The latter are given by the positions of the adlayer and substrate peaks with respect to the hexagonal coordinate system. Hence, the adlayer spacing can be calculated using the relationship $a_{\text{Cl}}/a_{\text{Au}}=[a_{\text{Cl}}^*/a_{\text{Au}}^*]^{-1}=[\sqrt{3}X]^{-1}$. The chloride surface density and coverage are given by $\Gamma=[a_{\text{Cl}}^2\sqrt{3}/2]^{-1}=2\sqrt{3}X^2a_{\text{Au}}^{-2}$ and $\theta=\Gamma a_{\text{Au}}^2\sqrt{3}/2=3X^2$. Typical chloride surface densities and coverages are slightly higher than $7 \times 10^{14} \text{ atoms/cm}^2$ and 0.5 ML, respectively.

With increasing electrode potential the peak position shifts to higher values as the adlayer is compressed. In Fig. 3(a) the chloride density Γ is shown as a function of potential E for two NaCl concentrations. At both concentrations Γ increases linearly with potential with the same slope. As visible in Fig. 3, the $\Gamma(E)$ curve does not depend on the direction of the potential change, indicating equilibrium conditions for chloride adsorption and desorption. From linear fits of the $\Gamma(E)$ curves we obtain a slope $\partial\Gamma/\partial E=(2.41 \pm 0.15) \times 10^{14} \text{ cm}^{-2} \text{ V}^{-1}$ (defined as electrocompression in Ref. 6). At all potentials the adlayer retains a hexagonal lattice with a fixed rotation angle of $30.0^\circ \pm 0.1^\circ$ relative to the substrate. Such aligned incommensurate phases have been reported in experimental² as well as in the theoretical¹⁰ studies.

The ordered phase exists only at very positive potentials, where the chloride surface density is high. At lower potentials, facilitating a lower surface density and a lower charge transfer, no diffraction peaks corresponding to an ordered adlayer structure could be observed. In this potential regime chloride most likely forms a disordered, fluidlike adlayer. It undergoes an order-disorder phase transition upon raising the potential to more positive values. At the potential where this phase transition is observed in the x-ray scattering experiment, traditional

electrochemical measurements, such as cyclic voltammograms¹¹ or differential-capacity curves,¹² show sharp peaks that suggest phase transitions in the anion adlayer. Similar sharp peaks were found to accompany the formation of ordered sulfate,¹³ iodide,^{4,6} and bromide¹⁴ adlayers on Au(111). They may be caused by discontinuous changes in the double-layer capacity and/or charge-transfer processes associated with these structural phase transitions. The upper limit of the stability range for the ordered adlayer cannot be observed by x-ray diffraction due to the oxidative roughening of the Au surface and the electrochemical formation of a soluble gold halide.

In solutions containing bromide ions an ordered hexagonal-close-packed adlayer is observed in the entire

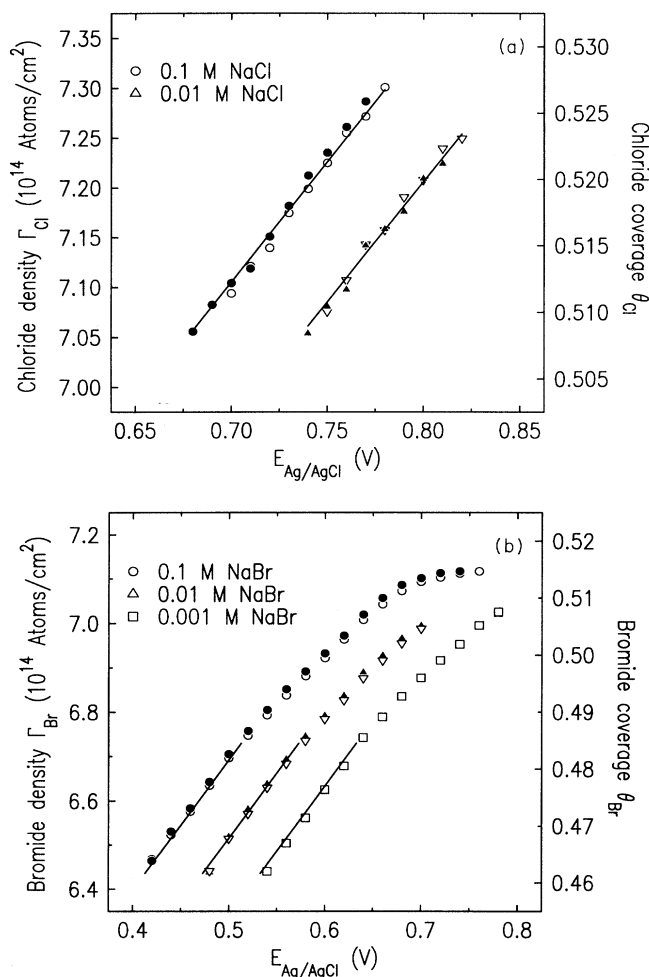


FIG. 3. Potential-dependent surface density $\Gamma(E)$ and coverage θ (relative to the Au lattice) of (a) chloride and (b) bromide in the ordered adlayer phase at various anion concentrations in the electrolyte. Data points were obtained by changing the potential in (a) 10-mV or (b) 20-mV steps starting from the potential of the ordered adlayer formation in positive (open symbols), and subsequently in negative direction (filled symbols). The electrocompression $\partial\Gamma/\partial E$ is obtained from fits of the linear region of the $\Gamma(E)$ curves (solid lines), the electroadsorption valency $\gamma = -1 \pm 0.2$ is obtained from the potential shift of the $\Gamma(E)$ curves with increasing NaCl concentration via the Nernst equation (Ref. 15).

potential range between 0.42 and 0.76 V (for 0.1M NaBr). Again, the adlayer is incommensurate and uniformly compresses with increasing potential as shown in Fig. 3(b). However, the $\Gamma(E)$ curves are linear only in the lower potential range. At more positive potentials the compressibility of the adlayer decreases until the density reaches a saturation value. The adatom spacing at this saturation density is 4.03 Å, i.e., close to the van der Waals diameter a_{vdW} of bromide. Unlike the ordered chloride layer, the bromide adlayer is not aligned along the $\sqrt{3}$ directions of the Au(111) substrate but deviates from the latter by a small potential-dependent angle φ_{rot} . A similar structure was observed for the ordered iodide monolayer on Au(111) at the most positive potentials.⁶ Differences between our results and previous *in situ* STM observations⁵ are related to the higher precision of the x-ray scattering measurements. A detailed description of bromide adsorption based on the results of a combined x-ray scattering STM study will be published elsewhere.¹⁴

The basic structural properties of the hexagonal adlayer phases of chloride, bromide, and iodide are summarized in Table I. All adlayers can be compressed up to an interatomic distance close to the van der Waals diameter a_{vdW} of the halide adsorbate. The electrocompression $\partial\Gamma/\partial E$ of the three species differs by only 30% indicating similar adsorbate-adsorbate interactions within the adlayers. From the potential shift of the $\Gamma(E)$ curves with the logarithm of the bulk electrolyte halide concentration we can evaluate the electroadsorption valency γ .⁶ The electroadsorption valency describes the potential dependence of the adsorption equilibrium and is related to the amount of charge transfer upon adsorption.¹⁵ For all three halide adsorbates γ is about -1 in the ordered phases, i.e., the adsorbates are almost completely discharged. The electroadsorption valency of bromide on gold was previously measured by electrochemical and optical methods at more negative potentials where the adlayer is disordered. Here considerably lower values, -0.4 to -0.76 , were found with the absolute value of γ rising with increasing potential.¹⁶ The latter may be consistent with the obser-

TABLE I. Structural properties (described in the text) of the incommensurate, hexagonal halide adlayers on Au(111). All data refer to the results of *in situ* x-ray scattering studies in electrolytes containing 0.1M chloride, bromide, and iodide.

	Chloride	Bromide	Iodide ^a
a_{vdW} (Å) ^b	3.52–3.80	3.70–4.00	3.90–4.24
a_{max} (Å)	4.03	4.24	4.47
Γ_{min} (10^{14} cm ⁻²)	7.10	6.42	5.79
$\partial\Gamma/\partial E$ (10^{14} cm ⁻² V ⁻¹)	2.41 ± 0.15	2.95 ± 0.07	1.98 ± 0.02
a_{max}/a_{vdW}	1.06–1.15	1.06–1.15	1.05–1.15
κ_{2D} (Å ² eV ⁻¹) ^c	4.65 ± 0.29	6.74 ± 0.17	5.40 ± 0.09
φ_{rot} (degrees)	0	3.3–4.7	2.8–3.4

^aData for the hexagonal, incommensurate phase of iodide on Au(111). Data for the uniaxial incommensurate ($p \times \sqrt{3}$) phase preceding the former at more negative potentials are shown in Ref. 6.

^bA. Bondi, J. Phys. Chem. **68**, 441 (1964).

^cCalculated from our data as described in Refs. 8 and 9 for a charge transfer $z = -1$.

vation of $\gamma = -1$ in the potential regime of the ordered adlayer.

The ordered halide adlayer is formed in a disorder-order transition at a critical surface density Γ_{\min} or average adatom distance a_{\max} . As shown in Table I, the ratio of this distance and of the van der Waals diameter of the adsorbate a_{\max}/a_{vdW} is approximately the same for all three halides (the absolute value of this ratio depends on the method by which the respective triplet of van der Waals diameters has been obtained). Previously, order-disorder phase transitions in (quasi) two-dimensional (2D) systems have been studied extensively by computer simulations using Monte Carlo techniques. A ratio of 1.12–1.19 has been calculated from simulations of a two-dimensional system of particles interacting via a Lennard-Jones potential,¹⁷ in agreement with our results. The average distance between the adsorbate and the first Au layer is about 2.4 Å for all halides according to previous *in situ* x-ray-reflectivity measurements.^{6,7} This, as well as spectroscopic results,¹⁸ suggest a predominantly covalent character of the Au-halide bond. However, the incommensurability of the halide lattice requires a more complicated delocalized bonding of these adlayers as has been proposed on the basis of vacuum experiments.¹

The energetics of the ordered adlayer is reflected by the lateral compressibility κ_{2D} . From our data, values for the halide-adlayer compressibilities in the range 4.5–7 Å² eV⁻¹ are obtained (Table I). This is higher than the compressibility of electrochemically deposited metallic monolayers [$\kappa_{2D} \approx 1-2$ Å² eV⁻¹ (Refs. 8 and 9)] but significantly lower than that of noble-gas monolayers on silver and graphite formed by adsorption from the gas phase [$\kappa_{2D} \approx 10-30$ Å² eV⁻¹ (Ref. 2)]. The compressibilities of the halide monolayers can neither be explained by the free-electron model valid for metal adlayers⁶ nor by models for physisorbed noble gases, where the

adsorbate-adsorbate interaction is modeled by pair potentials.² Using a Lennard-Jones pair potential (with length and energy parameters σ and ϵ approximated by a_{vdW} and the values of ϵ for halogen gases,¹⁹ respectively), we calculate halide-adlayer compressibilities which are five to ten times higher than the experimental values. A quantitative explanation of the observed compression and, in particular, of the especially high compressibility of bromide apparently requires a more sophisticated treatment of the adatom-adatom interactions in this interesting class of (quasi-) two-dimensional systems. In addition, substrate effects may cause a much richer phase behavior in some of these adsorbate systems. An example is provided by iodide on Au(111), where the hexagonal incommensurate adlayer is preceded by a uniaxial incommensurate ($p \times \sqrt{3}$) phase at more negative potentials.⁶

In summary, we have shown that chloride and bromide anions form ordered hexagonal-close-packed monolayers at the Au(111)-solution interface. These measurements are an example of *in situ* x-ray surface diffraction from low-*Z* adsorbates. The interatomic distance within the chloride and bromide as well as the structurally related iodide adlayers is a well-defined function of potential and indicates lateral interactions ranging between those of metallic and those of noble-gas monolayers.

Note added in proof. The lateral compressibilities calculated from Lennard-Jones pair potentials (see text above) depend strongly on the choice of the parameters σ and ϵ . Using values of σ which are 10–20 % larger than a_{vdW} , the experimental compressibilities of the halide adlayers can be reproduced.

The authors acknowledge support by the Divisions of Materials and Chemical Sciences, U.S. Department of Energy under Contract No. DE-AC02-76CH00016.

¹For recent reviews, see H. H. Farrell, in *The Chemical Physics of Solid Surfaces and Heterogeneous Catalysis*, edited by D. A. King, and D. P. Woodruff (Elsevier, New York, 1984), Vol. 36, Chap. 5; P. A. Dowben, *CRC Crit. Rev. Solid State Mater. Sci.* **13**, 191 (1987).

²J. Unguris, L. W. Bruch, E. R. Moog, and M. B. Webb, *Surf. Sci.* **87**, 415 (1979); **109**, 522 (1981).

³S. L. Yau, C. M. Vitus, and B. C. Scharadt, *J. Am. Chem. Soc.* **112**, 3677 (1990); R. Vogel and H. Baltruschat, *Surf. Sci.* **259**, L739 (1991).

⁴X. J. Gao and M. J. Weaver, *Am. Chem. Soc.* **114**, 8544 (1992); W. Haiss, J. K. Sass, X. J. Gao, and M. J. Weaver, *Surf. Sci.* **274**, L593 (1992).

⁵N. J. Tao and S. M. Lindsay, *J. Phys. Chem.* **96**, 5213 (1992).

⁶B. M. Ocko, G. M. Watson, and J. Wang, *J. Phys. Chem.* **98**, 897 (1994).

⁷J. Wang, A. J. Davenport, H. S. Isaacs, and B. M. Ocko, *Science* **255**, 1416 (1991); J. Wang, B. M. Ocko, A. J. Davenport, and H. S. Isaacs, *Phys. Rev. B* **46**, 10 321 (1992).

⁸O. R. Melroy *et al.*, *Phys. Rev. B* **38**, 10 962 (1988); *J. Electroanal. Chem.* **258**, 403 (1989).

⁹M. F. Toney, J. G. Gordon, M. G. Samant, G. L. Borges, and O. R. Melroy, *Phys. Rev. B* **45**, 9362 (1992).

¹⁰H. Shiba, *J. Phys. Soc. Jpn.* **46**, 1852 (1979); **48**, 211 (1980).

¹¹D. A. Scherson and D. M. Kolb, *J. Electroanal. Chem.* **176**, 353 (1984).

¹²A. Hamelin and J. P. Bellier, *J. Electroanal. Chem.* **41**, 179 (1973).

¹³O. M. Magnussen, J. Hageböck, J. Hotlos, and R. J. Behm, *Faraday Discuss. Chem. Soc.* **94**, 329 (1992).

¹⁴O. M. Magnussen, B. M. Ocko, J. Wang, and R. R. Adzic (unpublished).

¹⁵J. W. Schultze and K. J. Vetter, *J. Electroanal. Chem.* **44**, 63 (1973).

¹⁶R. Adzic, E. Yeager, and B. D. Cahan, *J. Electroanal. Chem.* **85**, 267 (1977); C. Nguyen Van Houg, C. Hinnen, and A. Rousseau, *ibid.* **151**, 149 (1983).

¹⁷F. F. Abraham, *Phys. Rep.* **80**, 339 (1981).

¹⁸P. Gao and M. J. Weaver, *J. Phys. Chem.* **90**, 4057 (1981).

¹⁹J. O. Hirschfelder, C. F. Curtis, and R. B. Bird, *The Molecular Theory of Gases and Liquids* (Wiley, New York, 1965), p. 1111.